Pulse-duration effect in nonsequential double ionization of Ar atoms

Shansi Dong,[1] Xiang Chen,[1] Jingtao Zhang,[1,*] and Xianghe Ren[2]
[1]*Department of Physics, Shanghai Normal University, Shanghai 200234, China*
[2]*School of Science, Qilu University of Technology, Jinan 250353, China*
(Received 18 January 2016; published 12 May 2016)

Nonsequential double ionization of Ar atoms in intense few-cycle laser pulses is studied by a classical ensemble method. The laser pulses are of trapezoidal shape with one cycle in both ramp on and ramp off. We obtain the cycle-resolved electron dynamics by increasing the optical cycles in the laser pulse one by one. We find that, at the higher laser intensity, the correlated-electron momentum distribution (CMD) in the three-cycle laser pulse exhibits two predominate structures in the first and third quadrants. They are formed by the electron pairs in which the second electron is knocked out by the returning electron in the second cycle. As the pulse duration increases, more electron pairs accumulate in the second and fourth quadrants of the CMDs. In these electron pairs, the second electron is first excited owing to collision with the returning electron and then is ionized by the laser field. By varying the peak intensity, we show the transition of the CMDs from anticorrelation to correlation in three-cycle laser pulses, which disproves that multiple collisions cause the transition.

DOI: 10.1103/PhysRevA.93.053410

I. INTRODUCTION

Electron-electron correlation (EEC) is very important in double ionization (DI) of atoms in intense laser fields [1]. First, the EEC is found to be a key to the nonsequential double-ionization (NSDI) process, in which the yield of the doubly charged ions is far higher than that based on the single-active-electron model [2]. Recently, the EEC process was found in sequential double ionization (SDI) [3]. The electron collision in DI provides a prototype of EEC which lies at the core of attosecond physics and thus has attracted much attention in the last two decades [4–6].

NSDI discloses an EEC process during photoionization in which one electron is first ionized by the laser field, then is accelerated by the laser field, is driven back near its parent ion when the electric field inverses, and finally collides with the parent ion and knocks out another electron [4]. Before ionization of the second electron, the first ionized electron may collide with the parent ion many times. These multiple collisions are found to produce hot electrons with energy higher than $2U_p$, where U_p is the ponderomotive energy [7,8]. After the second electron is ionized, the two electrons move inside the laser field and may collide again. This multiple-collision process is believed to cause the correlated electrons emitted back to back [9,10]. Studies on multiple collisions enrich our knowledge of DI. However, the effect of multiple collisions needs to be proved substantially.

NSDI in few-cycle laser pulses has been frequently studied, both experimentally and theoretically [5,11,12]. Because the electric strengths in opposite directions are not always equal to each other and vary greatly with the carrier-envelope (CE) phase, NSDI in few-cycle pulses depends on the CE phase [5]. This, in turn, provides a tool to control the electron correlation in NSDI [13]. The role of the CE phase relies on the pulse duration [14,15]. It was observed that changing pulse duration can control the breakage of chemical bonds [16]. Moreover, the ultrashort pulse diminishes the multiple collisions, so NSDI in a short pulse provides a clean EEC pattern of the correlated electrons [12]. This provides a way to identify the role of multiple collisions in NSDI.

The correlated-electron momentum distribution (CMD) is a principal tool for revealing the EEC effects in NSDI. The CMD denotes the number of electron pairs as a function of their momenta along the laser polarization. Many features, such as the fingerlike structure [17,18] and the cross-shaped structure [5], have been observed in CMDs. It has been shown that the CMDs transit from anticorrelation to correlation as the laser intensity increases [10]. This transition is attributed to the quantum tunneling effect [19], the multiple-collision effect [9,20–22], or the quantum interference effect [23]. However, a recent study shows that the transition reflects the influence of Coulomb repulsion between two electrons [24]. Further study is necessary to confirm the transition mechanism.

In this paper, using a classical ensemble method, we study the CMDs in n-cycle laser pulses with different pulse durations. The pulse envelope has a trapezoidal shape with one cycle in both the ramp on and the ramp off. In such laser pulses, the electric field in the pulse front and the subsequent flat top is kept unchanged for increasing n. This allows one to identify the ionization and collision processes in each optical cycle by increasing the cycle number one by one. We will show that, at a higher laser intensity, the CMD in the three-cycle laser pulse exhibits two predominate structures in the first and third quadrants, which are formed by the electron pairs when the second electron is knocked out by the returning electron in the second cycle. Subsequent optical cycles mainly produce low-energy electron pairs uniformly distributed in four quadrants of the CMDs. In these electron pairs, the second electron is first excited owing to the collision of the returning electrons and then is ionized by the laser field. By varying the peak intensity, we show the transition of the CMDs from anticorrelation to correlation in three-cycle laser pulses, where the multiple-collision process is absent.

II. SIMULATION METHOD

The simulation method we employed is based on the numerical integration of the time-dependent Newton equation, which has had great successes in dealing with NSDI in intense

*Corresponding author: jtzhang@shnu.eud.cn

laser fields [25,26]. This method reproduces many important features in NSDI [27]. Moreover, with the back-trajectory technique, this method can be used to track subcycle electronic dynamics during DI [28,29].

The light-free Hamiltonian of a two-active-electron atom can be written as (in atomic units)

$$H_e = \sum_{i=1,2}\left[\frac{\mathbf{P}_i^2}{2} - 2V_{sc}(r_i,a)\right] + V_{sc}(\mathbf{r}_1 - \mathbf{r}_2,b), \qquad (1)$$

where $\mathbf{r}_i$ and $\mathbf{p}_i$ denote, respectively, the position and momentum of the ith electron; V_{sc} stands for the soft-core Coulomb potential defined as $V_{sc}(\mathbf{r},c) = (r^2 + c^2)^{-0.5}$. In Eq. (1), a and b are smoothing parameters and are set to 1.50 and 0.05 for Ar atoms [25]. The initial position space collection of two electrons is populated by a Gaussian random series, ensuring the total kinetic energy is positive in Eq. (1). These electrons move freely for a while until they reach a stable position and momentum distribution. Then the ensemble of initial states is obtained, and an ensemble including 1.0×10^7 initial states is used in this paper.

The Hamiltonian of a two-active-electron atom in a laser pulse is given by $H = H_e + (\mathbf{r}_1 + \mathbf{r}_2)\cdot\mathbf{E}(t)$, where $\mathbf{E}(t)$ is the electric field of the laser pulse. It can be written as $\mathbf{E}(t) = E_0 f(t)\cos(\omega t + \phi)\hat{\mathbf{x}}$ for linear polarization, where E_0, ω, and ϕ are the laser amplitude, the frequency, and the CE phase, respectively; $f(t)$ denotes the pulse envelope, and $\hat{\mathbf{x}}$ is a unit vector along the x direction. The motion of two electrons in the laser field is governed by the canonical equation as

$$\frac{d\mathbf{r}_i}{dt} = \frac{\partial H}{\partial \mathbf{p}_i}, \quad \frac{d\mathbf{p}_i}{dt} = -\frac{\partial H}{\partial \mathbf{r}_i}. \qquad (2)$$

The above equation is solved by using the standard fourth- to fifth-order Runge-Kutta algorithm. At the end of the pulse, a DI event is counted when the energy of both electrons is greater than zero. A CMD is obtained statistically on all DI events.

According to the time interval between the collision of two electrons and ionization of the second electron, we classify the NSDI events as recollision impact ionization (RII) and recollision-induced excitation with subsequent field ionization (RESI) events. The RII event denotes the process in which the two electrons are ionized shortly after their collision, while the RESI event denotes the process in which the second electron is first excited by collision and then is freed by the laser field. In our simulations, the DI events with a time interval less than 0.1 optical cycle are counted as RII events.

III. DEPENDENCE OF CMDs ON PULSE DURATION

Using the above method, we calculate the CMDs of Ar atoms irradiated by few-cycle laser pulses with a wavelength of 800 nm. The pulse envelope is chosen as an n-cycle trapezoidal shape with one cycle in both the ramp on and the ramp off. In order to show variation of NSDI with the pulse duration, we deliberately choose a laser intensity that ensures significant DI occurs only from the second cycle. We choose the laser intensity to be 2.0×10^{14} W/cm^2, so the returning electron is energetic enough to release the second electron. After ionization, the electrons move inside the laser field and finally

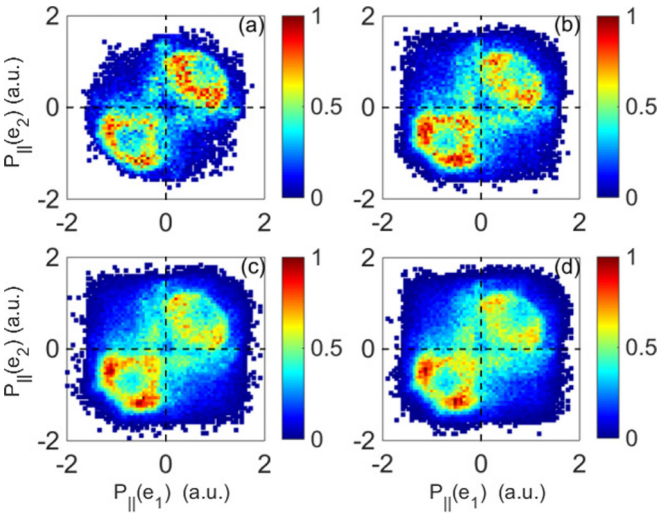

FIG. 1. CMDs of Ar atoms irradiated by n-cycle laser pulses of wavelength 800 nm and intensity 2.0×10^{14} W/cm^2 for (a) $n = 3$, (b) $n = 5$, (c) $n = 7$, and (d) $n = 9$.

have the following drift momentum:

$$\mathbf{P} = -\int_{t_0}\mathbf{E}(t)dt \simeq \frac{\mathbf{E}(t_0)}{\omega}, \qquad (3)$$

where t_0 denotes the time of ionization. This relation states that the drift momentum depends critically on the time of ionization but is independent of the pulse duration. So the drift momenta of the electrons obtained are the same for different cycle numbers.

Figure 1(a) depicts the CMD of Ar atoms irradiated by a three-cycle laser pulse. In this extremely short pulse, multiple collision is almost prohibited. Acceleration of the first ionized electron and the subsequent collision with the parent core occur in a time interval of about half an optical cycle. Moreover, after the second electron is ionized, they leave the laser field quickly. So the CMD reveals the momentum distribution after a single collision. The CMD exhibits bright regions highlighted from the blue background. The bright regions occur mainly in the first and the third quadrants, indicating most electron pairs are emitted outside the laser pulse in a side-by-side manner. The red arch-shaped structure in the first quadrant is brighter than that in the third quadrant. Figure 1(b) depicts the CMD in five-cycle laser pulses. The bright regions still occur mainly along the diagonal line. The difference from that in the three-cycle case lies in two aspects. One is that the red structure in the third quadrant becomes clearer than that in the first quadrant, contrary to the three-cycle case. The other is that the bright regions in the second and fourth quadrants become notable, indicating more electron pairs leave the laser pulse in a back-to-back manner. As the cycle number increases, the structures in the second and fourth quadrants become clearer and clearer, while the structures in the first quadrant become even less notable and turn into faint yellow regions, as shown in Figs. 1(c) and 1(d) for seven-cycle and nine-cycle laser pulses, respectively. A common feature in these CMDs is the red region in the third quadrant. This region is formed by the

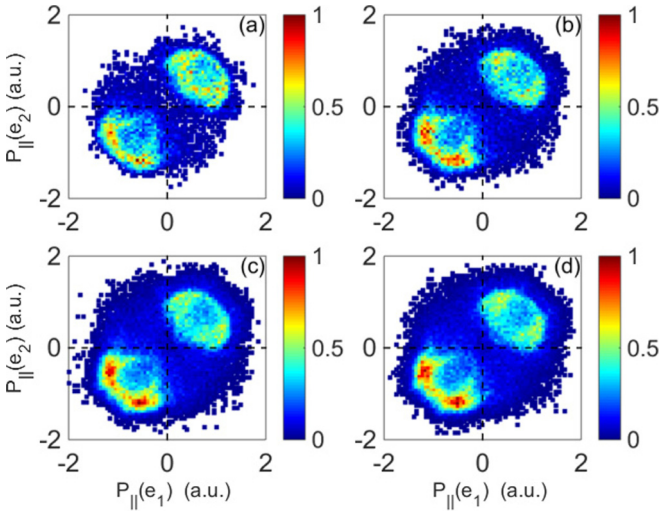

FIG. 2. CMDs from the RII process of Ar atoms in different n-cycle laser pulses. Other parameters are the same as those in Fig. 1.

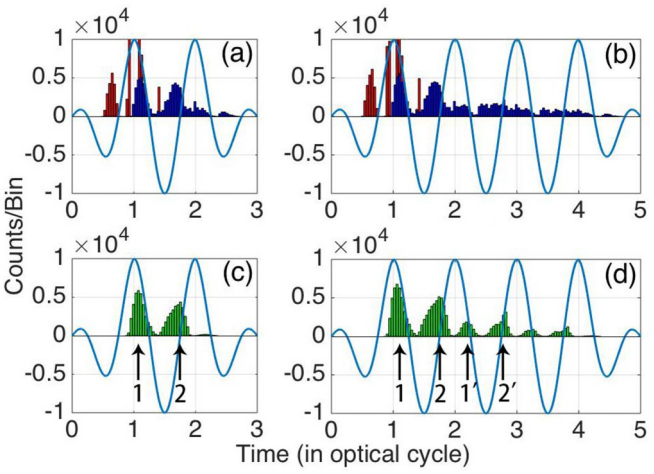

FIG. 3. Counts of the trajectories vs laser phase for ionization events of the first electron (red bars) and the second electron (blue bars) and recollision (green bars) events in (a) three- and (b) five-cycle laser pulses. The laser field is of intensity $2.0 \times 10^{14}\mathrm{W/cm^2}$ and wavelength 800 nm.

electron pairs released in the same half cycle and is kept almost unchanged in longer laser pulses.

Why do the bright areas in the second and fourth quadrants become notable as the laser duration increases? Physically, this indicates more electron pairs ejected outside the laser field back to back in longer laser pulses. In order to get an answer, we compare the CMDs of RII electrons in laser pulses of different durations. Figure 2 depicts the CMDs in laser pulses of $n = 3$, 5, 7, and 9. All CMDs exhibit two bright regions located in the first and third quadrants, indicating that most RII electron pairs are emitted outside the laser field in a side-by-side manner. The red structure in the third quadrant of all CMDs gets more noticeable as the pulse duration increases, which implies that more electrons become energetic in longer laser pulses since the red structures are located away from the center. However, for laser pulses including more than seven optical cycles, the CMDs remain almost the same [see Figs. 2(c) and 2(d) for $n = 7$ and 9, respectively]. This implies that the RII process stays the same in longer laser pulses and that the additional optical cycles do not release more RII electrons.

Excluding the contribution of the RII electrons from NSDI, the remaining part denotes the contribution of the RESI electrons. Hence, a comparison of Fig. 1 with Fig. 2 discloses the contribution of RESI electron pairs. It is easy to see two points. One is that the RESI electron pairs cluster mainly in the central region. The RII electron pairs form the high-energy structures of the CMD, and a blue valley near the central region is found in Fig. 2. This differs distinctively from that in Fig. 1, and the blue valley is compensated by the RESI electrons. The other point is that the bright areas in the second and fourth quadrants of the CMDs are formed mainly by the RESI electron pairs. Hence, we judge that the RESI electron pairs distribute near the central region and are equally distributed in four quadrants. This statement agrees well with the theoretical prediction [30]. The bright areas become notable in longer laser pulses, indicating that more electron pairs are released via the RESI mechanism in longer laser pulses. The physical reason is the excited electrons have more time to be ionized by the laser field.

Another duration-dependent phenomenon lies in the RII process. In Fig. 1(a), the red region is more notable in the first quadrant, while it becomes distinctive in the third quadrant in Fig. 1(b). Statistics data show that, in the five-cycle pulse, the number of electron pairs in the third quadrant is about 15% larger than that in the first quadrant, whereas in the three-cycle pulse, the number of electron pairs in the first quadrant is a little larger than that in the third quadrant. Since the laser pulse used in Fig. 1(b) differs from that in Fig. 1(a) by two additional optical cycles in the flat region, one may wonder why more electron pairs accumulate in the third quadrant in these two cycles.

In order to present substantial evidence, we count the number of DI events as a function of time. Statistical data show that ionization of the first electron begins with the second half cycle in the leading edge and exhibits two peaks in the second and third half cycles but occurs less in the following half cycles. Collision of two electrons and ionization of the second electron begin with the first half cycle in the pulse flat and exhibit double peaks in the first cycle of the pulse flat. This is the major process in a three-cycle pulse, as shown in Fig. 3(a). For five-cycle and longer laser pulses, more small peaks appear in the subsequent cycles. Generally, collision and ionization of the second electron lag behind ionization of the first electron by a half cycle, which is the time for the first electron to be accelerated and return.

Both the ionization and the collision of two electrons occur mainly in an optical cycle and exhibit two groups in the plots. These two groups, marked by 1 and 2, respectively, correspond to the predominate structures in the CMDs. Since the laser field is strong enough to govern the motion of the ionized electrons, the electrons in one group move in the same direction after they are ejected outside the laser field. According to this information, the electrons in the neighboring groups move in opposite directions, so the electrons in the two groups

form the two red regions in the CMDs. The correspondence is more straightforward in three-cycle laser pulses. The red arch-shaped structure in the first quadrant is formed by the electron pairs freed mainly in group 1, and that in the third quadrant is formed by the electron pairs freed mainly in group 2.

Figure 3 depicts the number of ionization and collision events via time in three-cycle and five-cycle pulses. The electric fields are also shown to identify the time correspondence. A comparison between the left column and the right column indicates that, besides the two major groups, the five-cycle plot exhibits additional small groups in the subsequent cycles. The group marked by $2'$ is a little more noticeable than that marked by $1'$. This causes the red region to be more distinctive in the third quadrant of Fig. 1(b).

IV. ROLE OF MULTIPLE COLLISIONS

In this section, we focus on the role of multiple collisions. Multiple-collision processes can be classified into two categories. In one the first ionized electron collides with the parent core many times before the second electron is ionized. This multiple-collision process is thought to be responsible for the production of electrons with energy higher than the classical limit, say $2U_p$. In the other kind of multiple-collision process the collision of two freed electrons in the laser field is responsible for the transition of CMDs from anticorrelation to correlation. The multiple-collision process is prohibited in ultrashort laser pulses with a duration shorter than four optical cycles [12]. So the laser pulses we used make it possible to identify the role of multiple collisions.

In order to identify the role of multiple collisions, we calculate the CMDs in three-cycle laser pulses of different intensities. Figure 4(a) depicts the CMD for a laser intensity of 0.75×10^{14} W/cm^2, which is illustrated by two bright dots located in the second and fourth quadrants. The CMD is anticorrelated. At such a lower laser intensity, the electron pairs are ionized mainly by the RESI process. As the laser intensity increases, as shown in Fig. 4(b) for 1.0×10^{14} W/cm^2, those bright dots become dim. Moreover, in contrast to a very dim area in the first quadrant, bright structures appear in the third quadrant. This CMD is only part of that in the long laser pulses [24] and is caused by the asymmetric distribution of the electric field. The two red dots in the third quadrant form the major structure. They expand and finally merge into an arch-shaped structure as the laser intensity increases further, as shown in Fig. 4(c) for 1.5×10^{14} W/cm^2. Meanwhile, the bright region in the first quadrant becomes more and more noticeable, as shown in Figs. 4(c) and 4(d). The CMD shown in Fig. 4(d) is correlated and indicates that most electron pairs are ejected in a side-by-side manner. This indicates that, as the laser intensity increases, the CMD transits from anticorrelation to correlation in three-cycle laser pulses, in which the multiple-collision process is absent. This confirms, that the Coulomb repulsion between two electrons causes the anticorrelated CMDs in lower-intensity fields, which is also supported by Zhou et al.'s study on He atoms [31]. It should be mentioned that in three-cycle laser pulses, the electric field distribution varies with the CE phase, and so does the CMD. All the CMDs are for the CE phase $\phi = 0$.

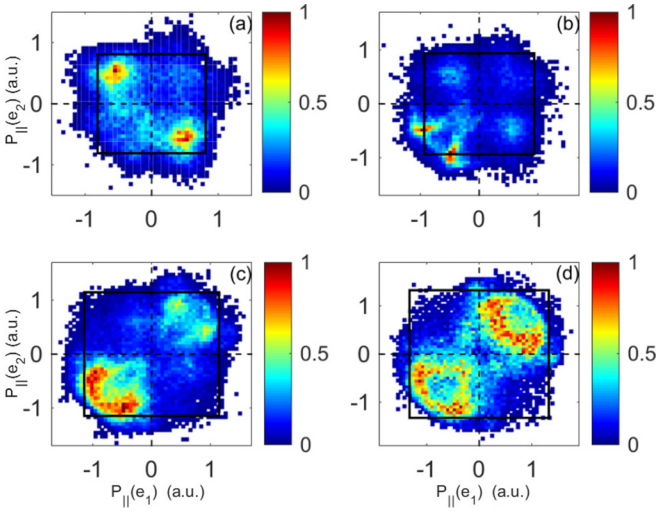

FIG. 4. CMDs in three-cycle laser pulses of different peak intensities: (a) 0.75×10^{14}, (b) 1.0×10^{14}), (c) 1.5×10^{14}, and (d) 2.0×10^{14} W/cm^2, respectively. The black square frame denotes the energy of $2Up$.

In Fig. 4, the black square frames denote an energy of $2U_p$, which is the classical limit of a free electron obtained from a laser field. The electron pairs located beyond the frame have energy exceeding this limit. Noticeable electrons are released with energy exceeding $2U_p$ in three-cycle laser pulses. This indicates some mechanisms beyond the multiple-collision process between the first electron released and the parent core. Further study is needed to discover the unknown mechanism.

V. CONCLUSIONS

Using a classical ensemble method, the NSDI of Ar atoms in few-cycle laser pulses was studied. The cycle-resolved electronic dynamics was identified by increasing the optical cycles in the laser pulses one by one. We found that the RII process produces energetic electrons that form the predominate structure in the CMDs and that the RESI process yields lower-energy electrons that form the structures around the center of CMDs. The number of RESI electrons becomes notable only in longer laser pulses. By increasing the peak intensity in three-cycle laser pulses, we showed the transition of the CMDs from anticorrelation to correlation, which disproves that multiple collisions cause the transition.

ACKNOWLEDGMENTS

This work is supported by the Chinese National Natural Science Foundation under Grants No. 11174304, No. 61475168, and No. 61307130 and Natural Science Foundation of Shanghai under Grant No. 15ZR1430600. J.Z. is sponsored by the Shanghai Gaofeng & Gaoyuan Project for University Academic Program Development.

[1] W. Becker, X. Liu, P. Ho, and J. H. Eberly, Rev. Mod. Phys. **84**, 1011 (2012).
[2] B. Walker, B. Sheehy, L. F. DiMauro, P. Agostini, K. J. Schafer, and K. C. Kulander, Phys. Rev. Lett. **73**, 1227 (1994).
[3] A. Fleischer, H. J. Worner, L. Arissian, L. R. Liu, M. Meckel, A. Rippert, R. Dorner, D. M. Villeneuve, P. B. Corkum, and A. Staudte, Phys. Rev. Lett. **107**, 113003 (2011).
[4] Th. Weber, H. Giessen, M. Weckenbrock, G. Urbasch, A. Staudte, L. Spielberger, O. Jagutzki, V. Mergel, M. Vollmer, and R. Döner, Nature (London) **405**, 658 (2000).
[5] B. Bergues, M. Kūel, N. G. Johnson, B. Fischer, N. Camus, K. J. Betsch, O. Herrwerth, A. Senftleben, A. M. Sayler, T. Rathje, I. Ben-Itzhak, R. R. Jones, G. G. Paulus, F. Krausz, R. Moshammer, J. Ullrich, and M. F. Kling, Nat. Commun. **3**, 813 (2012).
[6] A. N. Pfeiffer, C. Cirelli, M. Smolarski, R. Döner, and U. Keller, Nat. Phys. **7**, 428 (2011).
[7] J. S. Parker, B. J. S. Doherty, K. T. Taylor, K. D. Schultz, C. I. Blaga, and L. F. DiMauro, Phys. Rev. Lett. **96**, 133001 (2006).
[8] S. L. Haan and Z. S. Smith, Phys. Rev. A **76**, 053412 (2007).
[9] Y. Liu, L. Fu, D. Ye, J. Liu, M. Li, C. Wu, Q. Gong, R. Moshammer, and J. Ullrich, Phys. Rev. Lett. **112**, 013003 (2014).
[10] Y. Liu, S. Tschuch, A. Rudenko, M. Durr, M. Siegel, U. Morgner, R. Moshammer, and J. Ullrich, Phys. Rev. Lett. **101**, 053001 (2008).
[11] C. Huang, Y. Zhou, Q. Zhang, and P. Lu, Opt. Express **21**, 11382 (2013).
[12] T. T. Xu, S. Ben, T. Wang, J. Zhang, J. Guo, and X. S. Liu, Phys. Rev. A **92**, 033405 (2015).
[13] S. X. Hu, Phys. Rev. Lett. **111**, 123003 (2013).
[14] J. Zhang and Z. Xu, Phys. Rev. A **68**, 013402 (2003).
[15] J. Zhang, L. Bai, S. Gong, Z. Xu, and D.-S. Guo, Opt. Express **15**, 7261 (2007).
[16] X. Xie, E. Lotstedt, S. Roither, M. Schoffler, D. Kartashov, K. Midorikawa, A. Baltuska, K. Yamanouchi, and M. Kitzler, Sci. Rep. **5**, 12877 (2015).
[17] A. Rudenko, V. L. B. de Jesus, Th. Ergler, K. Zrost, B. Feuerstein, C. D. Schröter, R. Moshammer, and J. Ullrich, Phys. Rev. Lett. **99**, 263003 (2007).
[18] A. Staudte, C. Ruiz, M. Schoffler, S. Schossler, D. Zeidler, Th. Weber, M. Meckel, D. M. Villeneuve, P. B. Corkum, A. Becker, and R. Dorner, Phys. Rev. Lett. **99**, 263002 (2007).
[19] T. Shaaran, M. T. Nygren, and C. Figueira de Morisson Faria, Phys. Rev. A **81**, 063413 (2010).
[20] D. F. Ye and J. Liu, Phys. Rev. A **81**, 043402 (2010).
[21] X. L. Hao, W. D. Li, J. Liu, and J. Chen, Phys. Rev. A **83**, 053422 (2011).
[22] X. Y. Jia, X. L. Hao, D. H. Fan, W. D. Li, and J. Chen, Phys. Rev. A **88**, 033402 (2013).
[23] X. L. Hao, J. Chen, W. D. Li, B. Wang, X. Wang, and W. Becker, Phys. Rev. Lett. **112**, 073002 (2014).
[24] Z. Zhang, J. Zhang, L. Bai, and X. Wang, Opt. Express **23**, 7044 (2015).
[25] Q. Su and J. H. Eberly, Phys. Rev. A **44**, 5997 (1991).
[26] X. Wang, J. Tian, and J. H. Eberly, Phys. Rev. Lett. **110**, 073001 (2013).
[27] F. Mauger, C. Chandre, and T. Uzer, Phys. Rev. Lett. **105**, 083002 (2010).
[28] R. Panfili, S. L. Haan, and J. H. Eberly, Phys. Rev. Lett. **89**, 113001 (2002).
[29] S. L. Haan, L. Breen, A. Karim, and J. H. Eberly, Phys. Rev. Lett. **97**, 103008 (2006).
[30] B. Feuerstein, R. Moshammer, D. Fischer, A. Dorn, C. D. Schröter, J. Deipenwisch, J. R. Crespo Lopez-Urrutia, C. Höhr, P. Neumayer, J. Ullrich, H. Rottke, C. Trump, M. Wittmann, G. Korn, and W. Sandner, Phys. Rev. Lett. **87**, 043003 (2001).
[31] Y. Zhou, C. Huang, and P. Lu, Phys. Rev. A **84**, 023405 (2011).